Effective field theory for ^{4}He

J. M. Carmona,[1,2,*] S. Jiménez,[1,2,3,†] J. Polonyi,[4,5,‡] and A. Tarancón[1,2,§]
[1]*Departamento de Física Teórica, Universidad de Zaragoza, Zaragoza, Spain*
[2]*Instituto de Biocomputación y Física de Sistemas Complejos (BIFI), Corona de Aragón 42, Zaragoza 50009, Spain*
[3]*Dipartimento di Fisica, INFM and SMC, U. di Roma La Sapienza, P.le A. Moro 2, Roma I-00185, Italy*
[4]*Laboratory for Theoretical Physics, Louis Pasteur University, Strasbourg, France*
[5]*Department of Atomic Physics, Lorand Eötvös University, Budapest, Hungary*
(Received 29 November 2004; revised manuscript received 8 November 2005; published 3 January 2006)

We introduce an effective scalar field theory to describe the ^{4}He phase diagram, which can be considered as a generalization of the *XY* model which gives the usual λ transition. This theory results from a Ginzburg-Landau Hamiltonian with higher order derivatives, which allow one to produce transitions between the superfluid, normal liquid, and solid phases of ^{4}He. Mean field and Monte Carlo analyses suggest that this model is able to reproduce the main qualitative features of ^{4}He phase transitions.

DOI: 10.1103/PhysRevB.73.024501 PACS number(s): 67.90.+z, 05.10.Ln, 05.50.+q, 74.20.De

I. INTRODUCTION

Effective field theory models are widely used to describe phase transitions in condensed matter systems. The simplest example is that of the Ginzburg-Landau theory,[1] in which a "Hamiltonian" $H_{\mathrm{GL}}[\phi_i]$ depending on certain field variables ϕ_i and defined on the sites i of a lattice or at points $x, \phi(x)$, in its continuum formulation, may account for the description of first or second-order phase transitions.

The effective theory is not intended to be a microscopic theory at all. Instead, it makes use of the fact that critical phenomena are divided into universality classes which are determined by a few basic properties of the system only, such as the dimensionality of the space, the range of interactions, the number of components and the symmetry of the order parameter. The renormalization-group theory predicts that, within a given universality class, the critical exponents and the scaling functions are the same for all systems so that we can make use of the corresponding simpler effective theory to calculate such quantities.

In this context, the superfluid transition of ^{4}He, occurring along the λ-line $T_\lambda(P)$, where P is the pressure and T the temperature, belongs to the three-dimensional *XY* universality class.[2] Its order parameter is related to the complex quantum amplitude of helium atoms,[3] so that the O(2) field theory may serve as an effective description of this transition. In fact very good agreements between the critical exponents and scaling functions of this model and the experimental measurements of the λ transition of ^{4}He are found.[4]

Figure 1 shows the ^{4}He phase diagram in the (T,P) plane. The O(2) field theory is intended to describe this system in the vicinity of the λ transition, and strictly speaking only near T_c at zero pressure, because the model presents a temperature-driven transition only. The whole λ line is however expected to belong to the same universality class for $P \neq 0$. The transition lines between the liquid phases and the solid phase are experimentally observed to be of first order, with a finite entropy difference between the phases and the presence of a latent heat.[5]

In Fig. 1, the solid, superfluid and normal liquid phases meet at a single point, suggesting the presence of a Lifshitz point[6] in the ^{4}He phase diagram. In order to examine the critical behavior around this point, it would be very convenient to have an effective theory of this system containing all the three phases which meet there. This model should then be able to account for the transitions between the solid and the superfluid phases, solid and normal liquid phases, and superfluid and normal liquid phases.

We address the problem of finding such an effective theory in the present work. We take as an starting point the O(2) field theory, which describes the transition between the superfluid and normal liquid phases. In this theory, the superfluid phase corresponds to a *ferromagnetic* phase, in which there exists long-range order, while such an order is absent in the normal liquid phase, which corresponds to an unordered or *paramagnetic* phase. In order to generalize the O(2) field theory to a model including also a solid phase we should extend the regime of applicability of the effective theory towards shorter length scales below the lattice spacing of the solid.

What is the salient feature of the interactions at distances comparable to this lattice spacing? The periodic ordering in

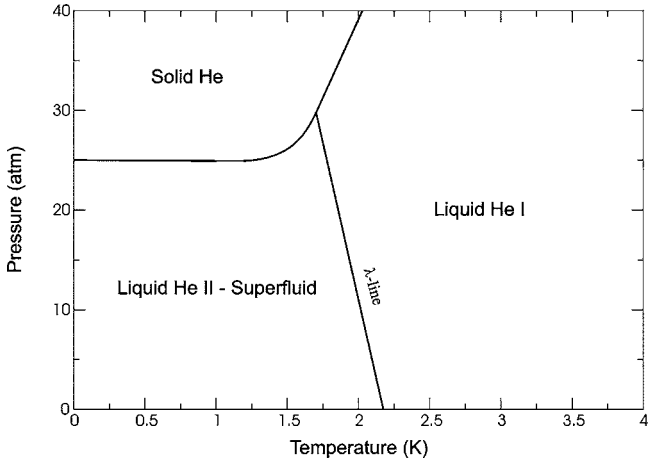

FIG. 1. Experimental pressure-temperature phase diagram for ^{4}He in the low temperature region. Two liquid phases, He I and superfluid He II, and a solid phase can be distinguished.

the ground state underlines the importance of the distance dependence of the forces acting in this scale regime. What kind of terms of the effective theory can reproduce an important distance dependence? The ultralocal polynomials of the field, without space-time derivatives, represent momentum (i.e., distance) independent interaction strength. When such a vertex is inserted into a graph then the distance dependence of the propagators can induce distance dependent vertex functions and therefore forces. But this is an indirect mechanism, the distance dependence actually originates from the propagators, the usual $O(p^2)$ part of the action. When the vertices carry explicit momentum dependence then the resulting forces should display more pronounced distance dependence. Therefore one suspects that terms with higher order derivatives might be the key to reproduce the solid phase.

The simplest vertex with higher order derivatives is quadratic in the field variable, meaning the modification of the free dispersion relation. If the dispersion relation turns out to be negative at a certain momentum, then the elementary excitation with such a momentum starts to condense in the vacuum. This condensation will be stopped and the system will be stabilized by the repulsive $O(\phi^4)$ interaction. Starting from the normal phase, the appropriately chosen mass term or the coefficient of the higher order derivative term will take us into the superfluid or the solid phase which will be called *modulated* phase. Note that the effective model may also contain an *antiferromagnetic* phase, in which the period length is the shortest possible scale of the theory. Such a phase will be however non-physical, since effective theories are supposed to give sensible physical descriptions only at energies lower than their energy cutoffs.

The universality argument of the normal-superfluid transition can be extended towards the solid phase at least in the leading order of the perturbation expansion. In fact, the perturbative, one-loop renormalizability at the Lifshitz point[7] provides us the universality at this order. It remains to be seen if the universality can be established nonperturbatively.

The heuristic reasoning above applies to any system with modulated ground state, such as the usual solid state crystal, Wigner-lattice of dilute electron gas and charge density wave state. But there is another consideration which makes the argument plausible in the context of ^{4}He, namely the existence of rotons. The higher order derivative terms of the effective action are present in either phases, their strength varies only when the phase boundaries are crossed. As we will see, the existence of rotons, the enhancement of elementary excitations at a given momentum which corresponds to a local minimum in the dispersion relation, is naturally reproduced by means of an action whose quadratic part in the field contains higher order derivatives. In fact, the rotons should correspond to the local minimum of the dispersion relation which becomes the absolute one as the superfluid-solid transition is crossed.

It is interesting to notice the formal similarity between the dynamics which drive the normal-to-superfluid and the normal-to-solid transitions. The former is spontaneous symmetry breaking where the potential energy reaches its minima at nontrivial, i.e., nonsymmetrical values of the field, at a nontrivial scale in the internal space. The symmetry spontaneously broken is an internal one and the dynamics is modified mainly in the IR domain. Similar phenomenon may take place in the external space, which leads to the modulated phase. If the dispersion relation reaches its minimum at nonvanishing momentum then particles with such momentum condense and the vacuum becomes modulated. This mechanism is driven by the derivative terms and modifies the dynamics mainly at length scales comparable with the inverse momentum of the particles condensing. The symmetry broken dynamically is an external one, rotations and translations.

The organization of our paper is the following. In Sec. II the effective theory for helium-4 is defined both in mathematical and physical terms. Section III is devoted to the mean field solution of the model. In Sec. IV we compare the mean field predictions with numerical Monte Carlo simulations of the system. We analyze its phase diagram and investigate the order of the transitions between phases. Finally, the conclusions are presented in Sec. V.

II. EFFECTIVE THEORY

Our model is an extension of the Ginzburg-Landau model in three dimensions for a complex scalar order parameter by adding higher order derivatives to the action,

$$S_c[\phi] = \int_x \left[\frac{1}{2}\partial_\mu \phi_j(x) \mathcal{K}(a^2\partial^2)\partial_\mu \phi_j(x) + \frac{1}{2}m_c^2 \phi_j(x)\phi_j(x) + \frac{\lambda_c}{4!}(\phi_j(x)\phi_j(x))^2 \right], \tag{1}$$

where $j=1, 2$, there is an implicit summation over repeated indices, and the kinetic energy contains the function

$$\mathcal{K}(z) = 1 + c_2 z + c_4 z^2. \tag{2}$$

The theory is regularized on a lattice of spacing a (the ultraviolet cutoff, which will be taken to be smaller than the period of the solid phase), so that the integral becomes $\int_x \to a^3 \Sigma_x$. One uses the dimensionless lattice field variable $\phi_x = \sqrt{a}\phi(x)$, and gets

$$S[\phi] = \sum_x \left[-\frac{1}{2}\phi_{j,x}\Delta\mathcal{K}(\Delta)\phi_{j,x} + m^2\phi_{j,x}\phi_{j,x} + \frac{\lambda}{4!}(\phi_{j,x}\phi_{j,x})^2 \right], \tag{3}$$

with $\Delta\phi_x = \Sigma_{\mu=1}^3(\phi_{x+\hat{\mu}} + \phi_{x-\hat{\mu}} - 2\phi_x)$, $m^2 = m_c^2 a^2$, $\lambda = a\lambda_c$.

Expanding $\Delta\mathcal{K}(\Delta)$ in $S[\phi]$, we obtain

$$S[\phi] = -\kappa_1 S_1 - \kappa_2 S_2 - \kappa_3 S_3 - \kappa_4 S_4 - \kappa_5 S_5 - \kappa_6 S_6 + \kappa \sum_x \phi_{j,x}\phi_{j,x} + \frac{\lambda}{4!}\sum_x (\phi_{j,x}\phi_{j,x})^2, \tag{4}$$

with the following definitions for the different terms and coefficients:

$$S_1 = \sum_{x,\mu} \phi_{j,x}\phi_{j,x+\hat{\mu}}, \quad \kappa_1 = 1 - 12c_2 + 123c_4, \tag{5}$$

$$S_2 = \sum_{x,\mu} \phi_{j,x}\phi_{j,x+2\hat{\mu}}, \quad \kappa_2 = c_2 - 18c_4, \tag{6}$$

$$S_3 = \sum_{x,\mu} \phi_{j,x}\phi_{j,x+3\hat{\mu}}, \quad \kappa_3 = c_4, \tag{7}$$

$$S_4 = \sum_{x,\mu<\nu} \phi_{j,x}(\phi_{j,x+\hat{\mu}+\hat{\nu}} + \phi_{j,x-\hat{\mu}+\hat{\nu}}), \quad \kappa_4 = 2c_2 - 36c_4, \tag{8}$$

$$S_5 = \sum_{x,\mu<\nu} \phi_{j,x}(\phi_{j,x+2\hat{\mu}+\hat{\nu}} + \phi_{j,x-2\hat{\mu}+\hat{\nu}} + \phi_{j,x+2\hat{\nu}+\hat{\mu}} + \phi_{j,x-2\hat{\nu}+\hat{\mu}}), \quad \kappa_5 = 3c_4, \tag{9}$$

$$S_6 = \sum_{x} \phi_{j,x}(\phi_{j,x+\hat{1}+\hat{2}+\hat{3}} + \phi_{j,x+\hat{1}-\hat{2}+\hat{3}} + \phi_{j,x-\hat{1}+\hat{2}+\hat{3}} + \phi_{j,x-\hat{1}-\hat{2}+\hat{3}}), \quad \kappa_6 = 6c_4, \tag{10}$$

$$\kappa = \frac{m^2}{2} + 3 - 21c_2 + 162c_4. \tag{11}$$

Physical interpretation

This effective model presents a number of parameters: m^2, λ, c_2, and c_4. m^2 and λ offer the possibility to have a broken symmetry, as in the standard Ginzburg-Landau Hamiltonian. Indeed, the polynomial

$$H(\varphi) = \frac{1}{2}r_0\varphi^2 + \frac{1}{4!}u_0\varphi^4, \quad u_0 > 0 \tag{12}$$

has two minima for $r_0 < 0$. The coefficient u_0 must be positive so that $\lim_{\varphi\to\pm\infty} H(\varphi) = +\infty$, which guarantees the stability of the minimum of $H(\varphi)$.

Therefore, $m^2 < 0$ and $m^2 > 0$ will give the broken and the paramagnetic phases, respectively, in the tree-level approximation. The parameter m^2 has to vanish linearly at the critical temperature, $m^2 \propto (T - T_c)$.

The other two parameters, c_2 and c_4, appearing in the higher order derivative part of the action, will be responsible for the emergence of the solid phase. Since making $c_2, c_4 \to 0$ in Eq. (1) gives the usual O(2) field theory, which describes the ^{4}He transition at $P=0$, we will associate the pressure to a linear combination of these two parameters, to be determined afterwards.

III. MEAN FIELD SOLUTION

The first, simplest step in determining the phase structure of the model is the tree-level solution which produces an inhomogeneous mean field in our case. Since this model is translational and rotational invariant in space we shall look for a mean field vacuum of the form

$$\begin{pmatrix} \phi_{1,x} \\ \phi_{2,x} \end{pmatrix} = \phi \begin{pmatrix} \cos(K^\mu x^\mu) \\ \sin(K^\mu x^\mu) \end{pmatrix}, \tag{13}$$

where the amplitude ϕ and the numbers $K^\mu, \mu = 1,2,3$, serve as variational parameters to minimize the action.

The action density, $s = S/L^2$, for an homogeneous, ferromagnetic vacuum ($K^\mu = 0 \,\forall\, \mu$) on a lattice L^d is obtained by minimizing

$$s_{FM} = \frac{m^2}{2}\phi^2 + \frac{\lambda}{4!}\phi^4, \tag{14}$$

$$s_{FM}^{\min} = \begin{cases} -3m^4/2\lambda, & m^2 < 0, \\ 0, & m^2 > 0. \end{cases} \tag{15}$$

In order to study the general case $K^\mu \neq 0$, we shall need the eigenvector of the lattice box operator,

$$\Delta\phi_{j,x} = -\hat{P}^2\phi_{j,x}, \tag{16}$$

where

$$\hat{P}^2 = 4\sum_\mu \sin^2\left(\frac{K^\mu}{2}\right). \tag{17}$$

One finds

$$-\Delta\mathcal{K}(\Delta)\phi_{j,x} = \mathcal{M}^2\phi_{j,x}, \quad \mathcal{M}^2 = \hat{P}^2(1 - \hat{P}^2c_2 + \hat{P}^4c_4). \tag{18}$$

Then the mean field action is

$$s = \frac{1}{2}(m^2 + \mathcal{M}^2)\phi^2 + \frac{\lambda}{4!}\phi^4, \tag{19}$$

with minimum

$$s_{\min} = -\frac{3(m^2+\mathcal{M}^2)^2}{2\lambda} \quad \text{at} \quad \phi^2_{\min} = -\frac{6(m^2+\mathcal{M}^2)}{\lambda}, \tag{20}$$

where $m^2 + \mathcal{M}^2 = m^2 + \hat{P}^2(1 - \hat{P}^2c_2 + \hat{P}^4c_4)$. This solution is valid only if $m^2 + \mathcal{M}^2 \leqslant 0$. The extrema of $m^2 + \mathcal{M}^2$ are reached at

$$\hat{P}^2_\pm = \frac{c_2 \pm \sqrt{c_2^2 - 3c_4}}{3c_4} \tag{21}$$

for $c_4 \neq 0$, and

$$\hat{P}^2_0 = \frac{1}{2c_2} \tag{22}$$

for $c_4 = 0$. However, $\hat{P}^2_+$ is a local minimum of Eq. (20), while $\hat{P}^2_-$ is a local maximum.

The local minimum $\hat{P}^2_+$ will be global or not depending on the specific values of c_2 and c_4. Moreover, $\hat{P}^2_+$ could be larger than 12, which is the maximum allowed value for $\hat{P}^2$ from its definition Eq. (17), or it could even be an imaginary number. It is therefore necessary to carry out a careful analysis of the absolute minima of Eq. (20), which will give us the different mean field vacua in the (c_2, c_4) plane.

A. Ordered mean field phases in the (c_2, c_4) plane

The conditions that will determine the global minimum of Eq. (20) for given (c_2, c_4) are

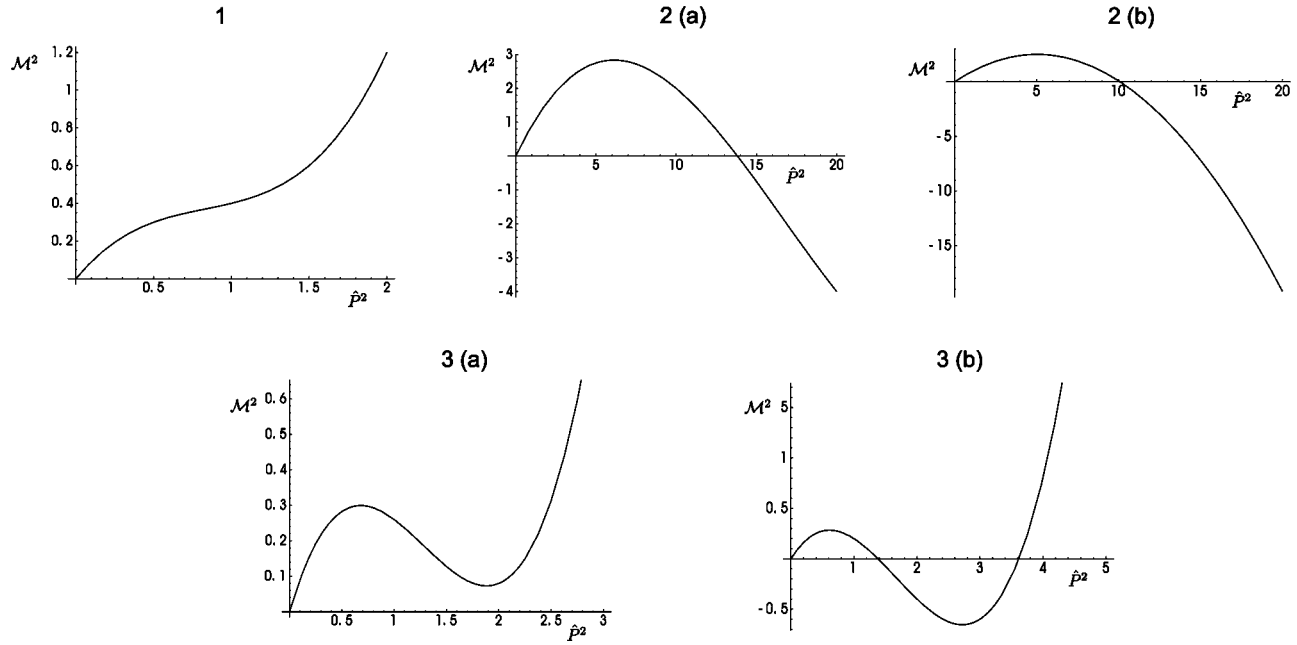

FIG. 2. $\mathcal{M}^2$ as a function of $\hat{P}^2$ for different values of (c_2, c_4) corresponding to the cases signaled in the text (from left to right, top to bottom): 1, 2(a), 2(b), 3(a), and 3(b).

$$\text{Existence of } \hat{P}_+^2 \Leftrightarrow c_4 < \frac{c_2^2}{3}, \tag{23}$$

$$\hat{P}_+^2 < 12 \Leftrightarrow c_4 > \max\left[\frac{c_2}{36}, \frac{1}{432}(-1+24c_2)\right], \tag{24}$$

$$\mathcal{M}^2(\hat{P}^2 = 12) < 0 \Leftrightarrow c_4 < \frac{1}{144}(-1+12c_2), \tag{25}$$

$$\mathcal{M}^2(\hat{P}^2 = \hat{P}_+^2) < 0 \Leftrightarrow c_4 < \frac{c_2^2}{4}. \tag{26}$$

In terms of these conditions, and supposing a value of m^2 such that $m^2+\mathcal{M}^2 \leqslant 0$, the phases (values of K^μ) which minimize Eq. (20) are (see Fig. 2 for an specific example of every case)

(1) If condition (23) does *not* hold, then Eq. (20) is minimized by $K^\mu = 0 \,\forall\, \mu$: *ferromagnetic* vacuum.

(2) If condition (23) *holds*, but condition (24) does *not* hold, then

(a) If condition (25) does *not* hold, then the minimum is again $K^\mu = 0 \,\forall\, \mu$: *ferromagnetic* vacuum.

(b) If condition (25) *holds*, then the global minimum of Eq. (20) is at $\hat{P}_+^2 = 12$ or $K^\mu = \pi \,\forall\, \mu$: *antiferromagnetic* vacuum.

(3) If both condition (23) *and* condition (24) *hold*, then

(a) If condition (26) does *not* hold, then the minimum is the *ferromagnetic* vacuum.

(b) If condition (26) *holds*, then the minimum of Eq. (20) is at the vector K^μ such that $\hat{P}^2 = \hat{P}_+^2$: we will call this a *modulated* phase.

Note that the plot in Fig. 2, case 3(a), corresponds to the dispersion relation of phonons and rotons (Landau spectrum[8]): we are in the ferromagnetic phase (superfluid phase) and there are two kind of excitations, at zero and different from zero momenta. At low energies, the curve is a straight line, corresponding to a phonon dispersion relation, while at higher energies, the spectrum deviates from a straight line, passing first through a maximum and then a minimum. The excitations with energies near this minimum are called rotons. The existence of the finite energy gap for rotons is crucial for the superfluidity in He II. The system enters into the solid phase when this gap tends to zero. The shape of the Landau spectrum has been confirmed by neutron-scattering experiments carried out in several different laboratories.[9]

From Eqs. (23)–(26) and the previous discussion, we can obtain the range of values of (c_2, c_4) for which the mean field vacuum is ferromagnetic (FM), antiferromagnetic (AF) or modulated (MOD). The result is summarized in Table I, and the phase diagram which results in the (c_2, c_4) plane is plotted in Fig. 3.

Let us now consider the order of the FM-MOD and MOD-AF transitions in this mean field approach. To do so,

TABLE I. Mean field phases for given (c_2, c_4) values, supposed that $m^2+\mathcal{M}^2 \leqslant 0$.

$c_2 \leqslant \frac{1}{12}$	FM	$\forall\ c_4$
$\frac{1}{12} \leqslant c_2 \leqslant \frac{1}{6}$	AF	if $c_4 < \frac{1}{144}(-1+12c_2)$
	FM	if $c_4 > \frac{1}{144}(-1+12c_2)$
$\frac{1}{6} \leqslant c_2 < \infty$	AF	if $c_4 < \frac{1}{432}(-1+24c_2)$
	MOD	if $\frac{1}{432}(-1+24c_2) < c_4 < \frac{c_2^2}{4}$
	FM	if $c_4 > \frac{c_2^2}{4}$

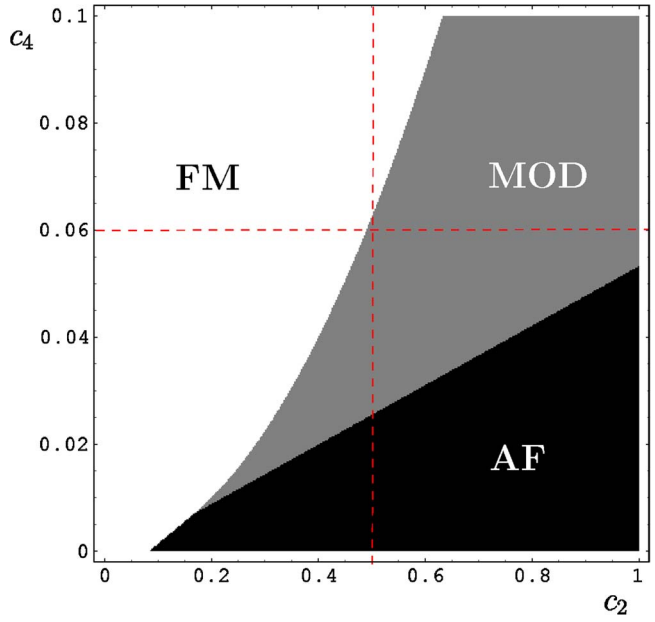

FIG. 3. (Color online) Mean field phase diagram in the (c_2, c_4) plane, supposing that $m^2+\mathcal{M}^2 \leqslant 0$ at every point of the plane. The black zone represents the AF phase, the grey zone is the MOD phase, and the white region, the FM phase.

we will study the variation of the minimum of the mean field action Eq. (20) along a line c_2=const. Let us take the line c_2=0.5 which is plotted vertically in Fig. 3. The value of $s_{\min}$ along this line depends on $\mathcal{M}^2$, which in turn depends on the value of $\hat{P}^2 \equiv \hat{P}_m^2$ which minimizes it. This value is $\hat{P}_m^2=12$, $\hat{P}_+$ and 0, respectively, for the antiferromagnetic, modulated and ferromagnetic phases, and is plotted in Fig. 4 along the c_2=0.5 line. From this figure one can see that $\hat{P}_m^2$ has a discontinuity when passing from the MOD to the FM phase. This seems to suggest that $s_{\min}$ is also discontinuous and that the transition FM-MOD will be first order. However, we will now see that this is not the case.

The value of $s_{\min}$ at the FM phase is given by [see Eq. (20), with $\mathcal{M}^2=0$]

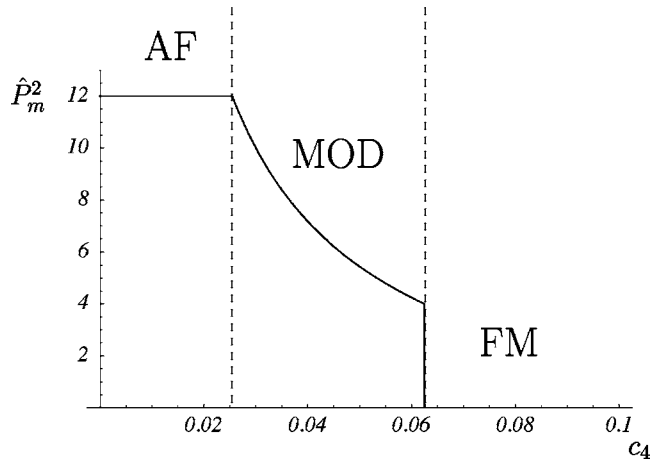

FIG. 4. Values of $\hat{P}^2$ which minimize $\mathcal{M}^2$ at c_2=0.5 as a function of c_4. They define the different vacua of the mean field action, as explained in the text.

$$s_{\min}^{FM} = -\frac{3m^4}{2\lambda}. \tag{27}$$

This value is independent of c_2 and c_4. The value of $s_{\min}$ at the MOD phase is given by Eq. (20), with $\mathcal{M}^2=\mathcal{M}^2(\hat{P}_+^2)$. This gives

$$s_{\min}^{MOD} = -\frac{[2c_2^3 + 2(c_2^2-3c_4)^{3/2} - 9c_2c_4 - 27c_4^2m^2]^2}{486c_4^4\lambda}. \tag{28}$$

However, when we evaluate this expression along the curve separating the FM and MOD phases, $c_4=c_2^2/4$, we obtain

$$s_{\min}^{MOD}(c_2, c_4=c_2^2/4) = -\frac{3m^4}{2\lambda} = s_{\min}^{FM}, \tag{29}$$

and there is no discontinuity in $s_{\min}$ between the two phases. Therefore, we conclude that the transition FM-MOD is a second-order transition.

In fact we could already have arrived to this conclusion just by a careful inspection of Fig. 2. The transition between the FM and MOD phases in Fig. 3 corresponds to the transition between cases 3(a) and 3(b) in Fig. 2. In case 3(a), $\mathcal{M}^2(\hat{P}_+^2)>0$ and the minimum of the action is at $\hat{P}_m^2=0(\mathcal{M}^2=0)$. In case 3(b), $\mathcal{M}^2(\hat{P}_+^2)<0$ and the minimum of the action is at $\hat{P}_+^2$. At the transition, $\mathcal{M}^2=0$ and there is no discontinuity in the action, but there is in its derivative with respect to the parameter of variation. The transition is second-order.

With respect to the AF-MOD transition, taking place at the curve $c_4=(-1+24c_2)/432$, it is evident from Fig. 4 that $s_{\min}$ should be continuous since $\hat{P}_m^2$ is continuous at this transition. In fact, again from Eq. (20),

$$s_{\min}^{AF} = -\frac{3(12-144c_2+1728c_4+m^2)^2}{2\lambda}, \tag{30}$$

and at the transition line

$$s_{\min}^{AF}\left(c_2, c_4=\frac{(-1+24c_2)}{432}\right) = s_{\min}^{MOD}\left(c_2, c_4=\frac{(-1+24c_2)}{432}\right) = -\frac{3(8-48c_2+m^2)^2}{2\lambda}. \tag{31}$$

This transition corresponds to that between the cases 2(b) and 3(b) in Fig. 2. In the first case, $\hat{P}_+^2>12$ and then the minimum is at $\hat{P}_m^2=12, \mathcal{M}^2(\hat{P}_m^2=12)<0$. When we approach the modulated phase then $\hat{P}_+^2 \to 12$. At the transition $\hat{P}_+^2=12$ and therefore $\mathcal{M}^2$ changes in a continuous way between the two phases. In this case the derivative of $\mathcal{M}^2$ is also continuous.

Finally, the transition between the AF and the FM phases in the second region of Table I $\left(\frac{1}{12} \leqslant c_2 \leqslant \frac{1}{6}\right)$, turns out to be also continuous, in spite of the fact that $\hat{P}_m^2$ jumps from 12 to 0 at the line $c_4=(-1+12c_2)/144$ since

$$s_{\min}^{AF}\left(c_2, c_4 = \frac{(-1+12c_2)}{144}\right) = -\frac{3m^4}{2\lambda} = s_{\min}^{FM}. \tag{32}$$

This can again be understood as the transition between cases 2(a) and 2(b) in Fig. 2, when we pass from $\mathcal{M}^2=0$ at the minimum of the action in the first case, to $\mathcal{M}^2<0$ in the second case. The change in $\mathcal{M}^2$ is then continuous, but its derivative is discontinuous.

In conclusion, all the transition lines in Fig. 3 turn out to be continuous transitions. At the FM-AF and FM-MOD transitions, when there is a jump in $\hat{P}_m^2$, the derivative of the action with respect to the parameter of variation in the (c_2, c_4) plane is discontinuous, while this derivative is continuous at the AF-MOD transition.

B. Complete mean field phase diagram

In the previous analysis we have made the assumption that m^2 was such that $m^2+\mathcal{M}^2 \leqslant 0$, which guarantees that we are in the broken phase, i.e., $\phi_{\min}^2 > 0$ [see Eq. (20)]. If this condition does not hold then the minimum of the action (19) is at $\phi=0$ and we are in the paramagnetic (PM) phase. This happens at a different value of m^2 depending on which ordered phase is considered:

$$m^2 \leqslant -\mathcal{M}^2 \Leftrightarrow \begin{cases} \text{FM phase}, & m^2 \leqslant 0, \\ \text{AF phase}, & m^2 \leqslant -\mathcal{M}^2(12), \\ \text{MOD phase}, & m^2 \leqslant -\mathcal{M}^2(\hat{P}_+^2). \end{cases} \tag{33}$$

In the three dimensional plane (m^2, c_2, c_4) we will have then four different phases: PM, AF, FM, and MOD. As we argued in Secs. I and II, we are interested in the physical region containing only FM, PM and MOD phases, which will represent the superfluid, normal liquid and solid phases, respectively, as a function of two parameters: m^2, which would correspond to the temperature T, and a combination of c_2 and c_4, which would correspond to the pressure P. Taking c_4 proportional to c_2 with an adequate slope gives us a section in the (c_2, c_4) plane represented in Fig. 3 where the qualitatively correct phase diagram appears: a FM phase followed by a MOD phase. The exact value of the slope is arbitrary, and we make the choice $c_4=0.25c_2$ so that the transition line between the MOD and FM phases is located at $c_2=1$. The complete phase diagram we get in this way is shown in Fig. 5 in the (m^2, c_2) plane. Note that this physical region may not be stable under renormalization group (RG) transformations. Under these transformations, which keep the physics fixed (unmodified long distance behavior), the period length will appear shorter when expressed in lattice spacing units. This means that they will in general connect the MOD phase with an antiferromagnetic phase, but with a quite complicated blocked action containing much more parameters than simply c_2 and c_4. Therefore the nonphysical AF phase which our simple effective model contains will not be connected by RG transformations with the physical region and we can safely discard this phase and its vicinity from our analysis.

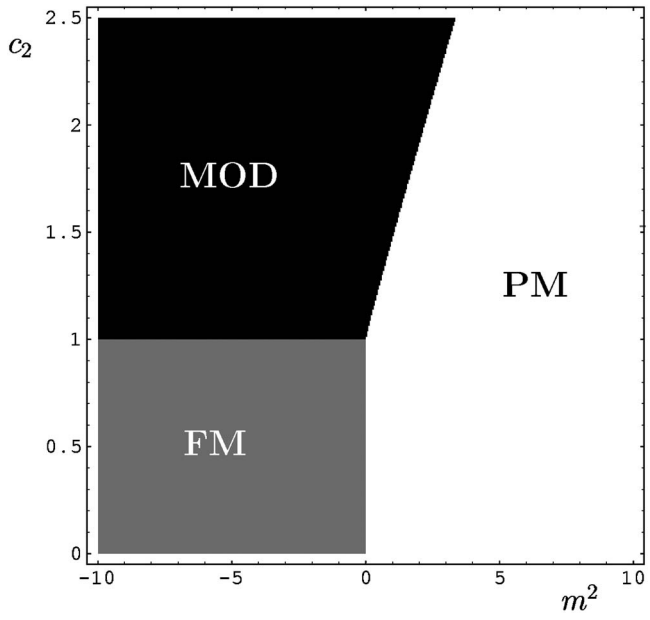

FIG. 5. Mean field phase diagram in the (m^2, c_2) plane, where at every point $c_4=0.25c_2$. Here the phases are PM (white region), FM (grey region), and MOD (black region).

It is easy to see that the transitions from an ordered phase (FM or MOD) to the paramagnetic phase are also continuous. The action inside the PM phase is 0 in the mean field approximation while in the FM and the MOD phases it is given by Eq. (19). However, the transition lines to the PM phase are just the regions of the parameter space where $m^2+\mathcal{M}^2=0$ and consequently the action is vanishing.

IV. MONTE CARLO SIMULATION OF THE MODEL

The preceding mean field study is qualitative only due to the absence of fluctuations. In order to estimate this error and to have a more reliable phase structure a numerical simulation of the model was performed as well. We considered a three dimensional cubic lattice of side L with periodic boundary conditions and studied the model Eq. (4) as a function of the two parameters m^2 and c_2, taking $\lambda=0.1$ and $c_4=0.25c_2$ as fixed values, in lattices $L=6,8,12,16,24$ with a Monte Carlo simulation. The algorithm was a standard Metropolis, and the errors were computed with a jack-knife method. In the largest simulations, we performed up to 50 million of full-lattice sweeps (measuring every 5 sweeps). We checked that the autocorrelation times were small with respect to the number of measurements performed for every lattice size.

A. Observables and the phase diagram

In order to identify the possible inhomogeneous condensates we write the field variable ϕ_x in terms of its Fourier transform,

$$\phi_x = \sum_K e^{iKx}\tilde{\phi}_K, \quad \tilde{\phi}_K = \frac{1}{V}\sum_x e^{-iKx}\phi_x, \tag{34}$$

where $Kx \equiv K^\mu x^\mu$, and there is summation over the repeated index μ. The possible values of K on each lattice direction

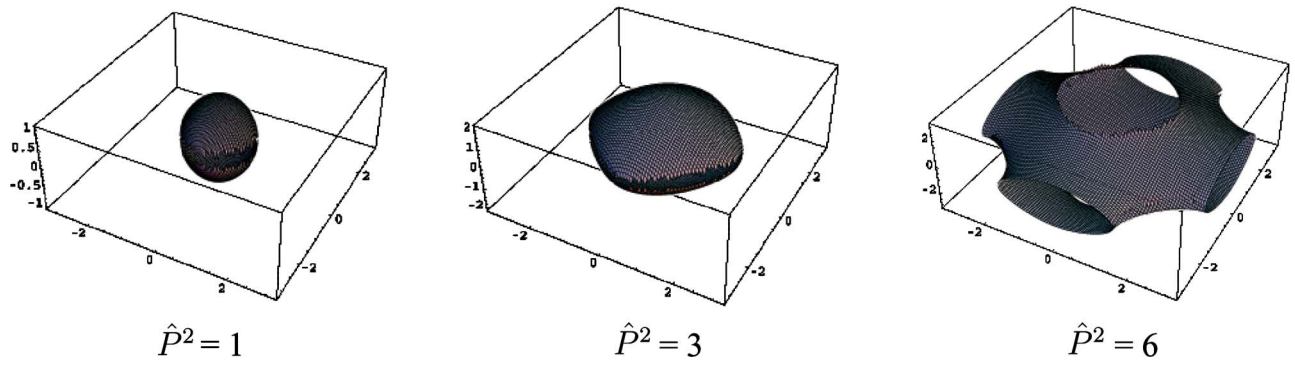

FIG. 6. (Color online) Surfaces in K space with the same $\hat{P}^2$, Eq. (17), for three different values $\hat{P}^2=1,3,6$.

are $(2\pi/L)n$, with $n=0,\ldots,L-1$. The magnetization corresponding to the wave-vector K is defined as the magnitude of the Fourier coefficient,

$$M_K = \sqrt{\|\tilde{\phi}_K\|^2}. \tag{35}$$

Our mean field solutions are pure Fourier modes, i.e., such that $\|\tilde{\phi}_K\|^2=0\,\forall K \neq \pm K_0$ for a certain K_0 which minimizes the action, and we introduce the corresponding momentum square as

$$\hat{P}^2 = 4\sum_\mu \sin^2\left(\frac{K_0^\mu}{2}\right). \tag{36}$$

$\hat{P}^2$ is the only combination of the components of the wave-vector K_0 appearing in the mean field solution. But this means that all different K configurations with the same value of $\hat{P}^2(K)$ are degenerated in energy. The degree of this degeneration naturally may depend on the value of $\hat{P}^2$. The surface in K space which corresponds to a given value of $\hat{P}^2$ is depicted in Fig. 6 for three different values $\hat{P}^2=1,3,6$.

The configurations are not single Fourier modes of the mean field type in the Monte Carlo simulation. A possible generalization of $\hat{P}^2$ is the average momentum square over all modes,

$$\overline{\hat{P}^2} \equiv 4\sum_\mu \sum_K \|\tilde{\phi}_K\|^2 \sin^2\left(\frac{K^\mu}{2}\right). \tag{37}$$

Another useful observable is the energy or in general any of the eight terms (or any linear combination of them) appearing in Eq. (4). Considering the energy as a function defined on the plane (m^2, c_2), the direction of the fastest change at a transition will be the one orthogonal to the transition line. Since the FM-MOD and FM-PM lines are almost horizontal and vertical in the parameter space, respectively, we considered the coefficients of c_2 and m^2 in S. Both linear combinations proved also to give a good signal for the MOD-PM transition. They can be read from Eqs. (4)–(11):

$$S_m \equiv \frac{1}{2}\sum_x \phi_{j,x}\phi_{j,x}, \tag{38}$$

$$S_c \equiv 56.25S_1 - 10.5S_2 + 0.75S_3 - 42S_4 + 9S_5 + 6S_6 - 39S_m. \tag{39}$$

These energies are also the appropriate ones to extrapolate the mean values of observables in an interval around a certain simulation point by means of a Ferrenberg-Swendsen reweighting method.[10] The observables Eqs. (35) and (37), together with the appropriate energy terms were measured in Monte Carlo simulations.

We performed two different kinds of simulations. First we swept the whole parameter space by fixing the value of one of the two parameters (c_2 or m^2), varying dynamically the other one in small steps (typically 10^{-3}) and measuring observables after a number of iterations (around 5000 Monte Carlo steps). This procedure allows us to locate the transition point by means of the rapid changes experienced in the different observables. We call this kind of simulation an *hysteresis* owing to the typical signs of metastability observed when crossing a first order transition (see Figs. 9 and 10 below). Once the phase diagram had been outlined we performed better statistics simulations at fixed values of the parameters at the transition lines to get a deeper insight into the properties of these transitions.

Figure 7 shows the observed phase transitions in an $L=16$ simulation, together with the mean field lines. One can see that the Monte Carlo results agree well with the mean field phase diagram. It is interesting to see that near the point where all phases meet, the slopes of the different transitions are similar to those of the helium phase diagram, see Fig. 1, after making the correspondence of the MOD, FM and PM phases to the solid, liquid He II and liquid He I phases, respectively (but note that the model does not pretend to give the exact slopes of the transition lines). This effective model seems therefore to give a good description of the helium phase diagram around the Lifshitz point when c_2 and m^2 are considered to be proportional to the pressure and the relative temperature, respectively. In the following section we study the nature of the phase transitions by using a Monte Carlo simulation and confirm that, in contrast to what we saw in the mean field analysis, they are of the same type as those of helium.

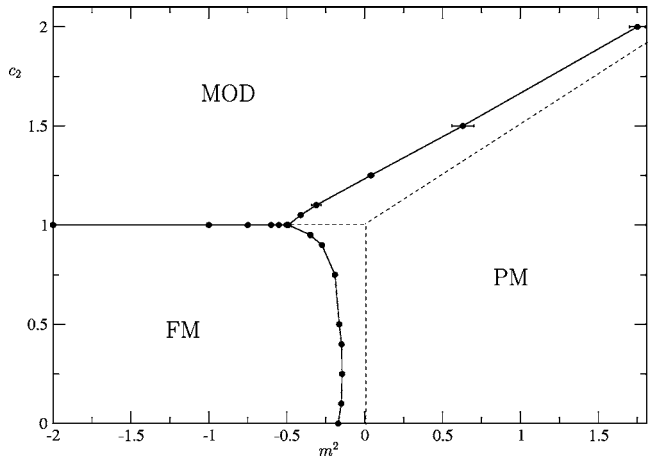

FIG. 7. Monte Carlo phase diagram for an $L=16$ lattice (continuous line and dots) versus mean field phase diagram (dashed line). Error bars which are not shown are smaller than the size of the points.

B. Phase transitions

1. FM-PM transition

The FM-PM transition is clearly second order, as we will show by calculating its critical exponents. This behavior is expected in order to reproduce the λ-line that separates the liquid He I and He II states in the phase diagram of ^{4}He.

Here the order parameter is the standard magnetization M_0 and one can perform the usual finite size scaling analysis in order to extract critical exponents and critical temperatures. A good choice for the scaling variable is the correlation length. In a finite size lattice it can be defined using a second moment method[11] as

$$\xi = \left(\frac{M_0^2/M_{K_m}^2 - 1}{4 \sin^2(\pi/L)} \right)^{1/2}, \tag{40}$$

where M_0^2 and $M_{K_m}^2$ are defined in Eq. (35), and $K_m = (2\pi/L, 0, 0)$ is the minimum wave vector compatible with the periodic boundary conditions.

For an operator O that diverges as $|t|^{-x_O}$ where t is the reduced temperature the mean value at a temperature T in a lattice of size L can be written in the critical region by means of the finite-size scaling ansatz[12] as

$$O(L,T) = L^{x_O/\nu}(F_O[\xi(L,T)/L] + O(L^{-\omega})), \tag{41}$$

where F_O is a smooth scaling function and ω is the universal leading correction-to-scaling exponent. In order to eliminate the unknown F_O function we use the method of quotients[13,14] where one studies the behavior of the operator of interest in two lattice sizes, L and rL,

$$Q_O = O(rL,t)/O(L,t) \tag{42}$$

and one chooses a value of the reduced temperature t such that the correlation-length in units of the lattice size is the same in both lattices. This temperature can be considered as the apparent transition point for the size L. One obtains easily

$$Q_O\big|_{Q_\xi = r} = r^{x_O/\nu} + O(L^{-\omega}). \tag{43}$$

We used the quotient method for pairs of lattices of sizes L and $2L$ and determined the values of the parameters (m^2, c_2) where the ξ/L curves cut each other. This is shown in Fig. 8 for $c_2=0.5$ and $L=8$, 12, 16, 24. The critical exponent ν ($\xi \sim |m^2 - m_c^2|^{\nu}$) was measured by using $\partial_{m^2}\xi$ ($\partial_{m^2}\xi \sim |m^2 - m_c^2|^{\nu+1}$) as the observable O of the quotient method and the apparent exponents together with the transition points are shown in Table II. The calculation of the scaling corrections and the exact extrapolation of the critical point and exponents have not been carried out since our intention was just to check that the transition belongs to the university class of the XY model in 3 dimensions (which corresponds to $c_2=0$). More precise calculations of critical exponents would require the use of update algorithms with smaller autocorrelation times in the vicinity of a continuous transition than the standard Metropolis, such as a single-cluster algorithm (for the problematics of the application of these algorithms to the standard Ginzburg-Landau model see, e.g., Ref. 15). For us it is enough to confirm that the values of the exponent ν re-

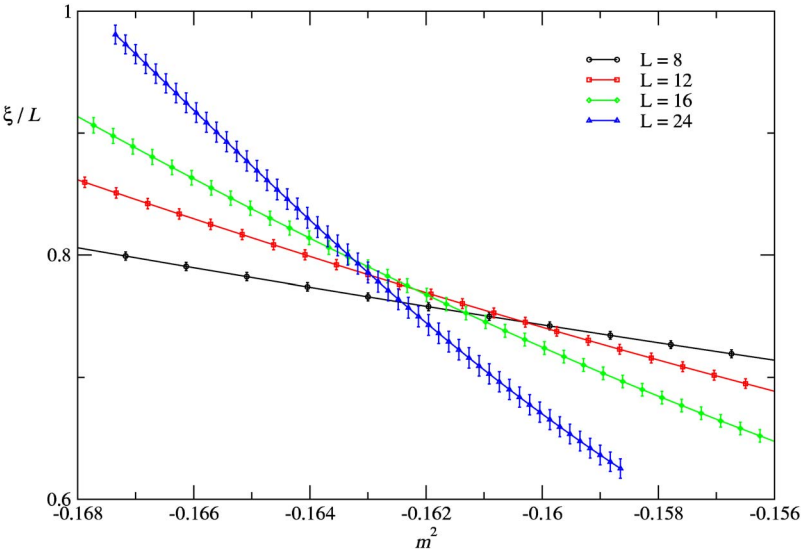

FIG. 8. (Color online) ξ/L for $c_2=0.5$ and lattice sizes $L=8$, 12, 16, 24.

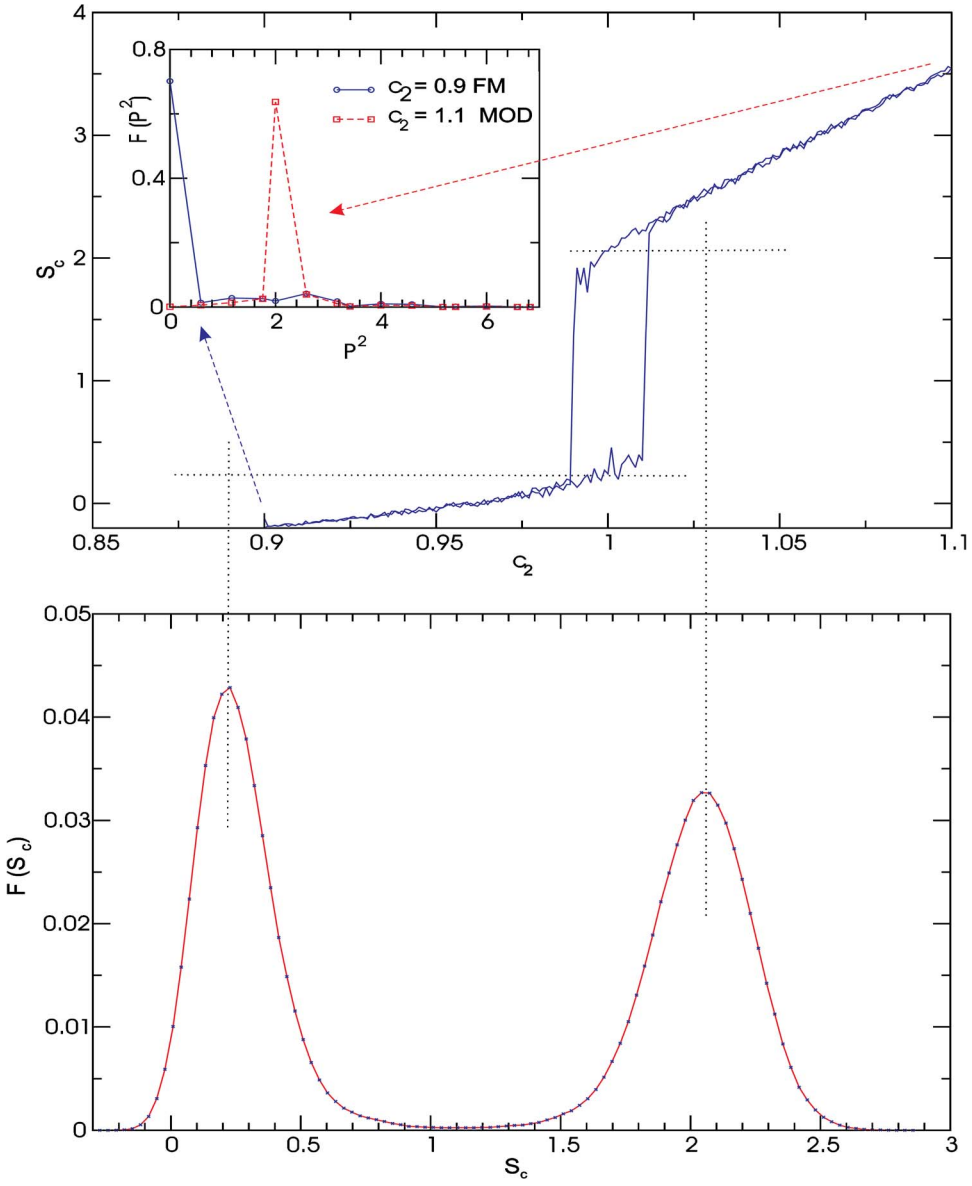

FIG. 9. (Color online) Top: Hysteresis cycle in c_2. Figure shows S_c, Eq. (39), versus c_2 for $m^2=-0.55$ in an $L=8$ lattice. *Inset*: $\hat{P}^2$ distribution, Eq. (37), at both sides of the transition for the same run as in the main plot. Inside the FM phase $F(\hat{P}^2)$ has a peak in $\hat{P}^2=0$, while when crossing to the MOD phase the peak changes its position to $\hat{P}^2\sim 2$. Bottom: Histogram of S_c for a run with fixed parameters $c_2=1.0, m^2=-0.55$, in an $L=8$ lattice. Dotted lines mark the position of the peaks of the histogram in the hysteresis plot. The double-peak form of the histogram shows clearly the first order character of the FM-MOD transition.

ported in Table II turn out to be fully compatible (as expected) with that of the XY model in $3d$,[16] 0.67155(27).

2. FM-MOD transition

Hysteresis-type simulations along fixed $m^2<0$ lines show metastability signs, indicating a first order character of the FM-MOD transition at $c_2\to 1$. This is shown in the top part of Fig. 9. In the small inset of this figure the differences in the distribution of $\hat{P}^2$ are shown at both sides of the transition. This distribution is peaked at $\hat{P}^2=0$ in the FM phase, and changes to a value clearly different from zero (around 2) when crossing the transition line to the MOD phase, as expected from the mean field calculation (which gives $\hat{P}^2=2$ at the transition point for all values of m^2).

TABLE II. m_c^2 determined by the intersection of the correlation lengths measured in two lattices of sizes L and $2L$ and the apparent critical exponent ν obtained from the quotient method applied to the same $(L,2L)$ pairs.

L	m_{cL}^2	ν_L
6	−0.1562(6)	0.663(10)
8	−0.1613(4)	0.656(12)
12	−0.1629(5)	0.678(17)

An hysteresis might be observed for second order transitions as well when it indicates the sudden increase of the relaxation time around the critical point. In order to exclude this possibility we looked into a feature characteristic of the first order transitions only, the appearance of double-peaks in the histogram of important observables. The histogram of the energy, shown in the bottom part of Fig. 9, corresponds to an $L=8$ simulation at $c_2=1.0$, $m^2=-0.55$. Such a double-peak structure is not expected when the fluctuations around the mean field solution of Sec. III A are considered at one-loop level. It is well known that fluctuations may change the transition from second to first order, especially for the so-called

weak first order transitions.[17] A first order character is indeed what is expected for a liquid-solid transition where there is a finite latent heat.

Finally, Fig. 7 shows that the FM-MOD transition line obtained in the numerical simulation is almost horizontal, here in agreement with the mean field calculation, and also with the experimental phase diagram Fig. 1.

3. MOD-PM transition

The solid to ordinary liquid transition is also first order in ^{4}He. Our mean field solution predicted however a continuous transition. But this is again changed by the effect of fluctuations, as the numerical simulation reveals.

The top part of Fig. 10 shows some hysteresis plots for different lattice sizes at $c_2=1.5$. Their form shows clear signs of a metastability at the MOD-PM transition. But notice however the appreciable finite size dependence on the location of the apparent transition point. This effect may be understood by looking at the shape of the distributions of $\overline{\hat{P}^2}$ of the $L=8$ and $L=16$ lattices, shown in the middle part of Fig. 10. The $L=16$ $\overline{\hat{P}^2}$ distribution shows a peak at the value of the mean field prediction in the modulated phase (2.27 for $c_2=1.5$). The $L=8$ distribution is however extended in a larger range with a maximum at a lower value of $\overline{\hat{P}^2}$. In fact, the spacing between Fourier modes is $2\pi/L$, a finite number on a finite lattice, which implies that the measured values of $\overline{\hat{P}^2}$ are also discretized. The mean field value lies between two of the allowed values for the $L=8$ size, producing a competition between different kinds of modulation in the system. This is of course a finite size effect which disappears for large lattices.

The $\overline{\hat{P}^2}$ distribution is spread in the paramagnetic phase. This is clearly seen in Fig. 10, middle, for $L=16$ while the spreading is weaker for $L=8$.

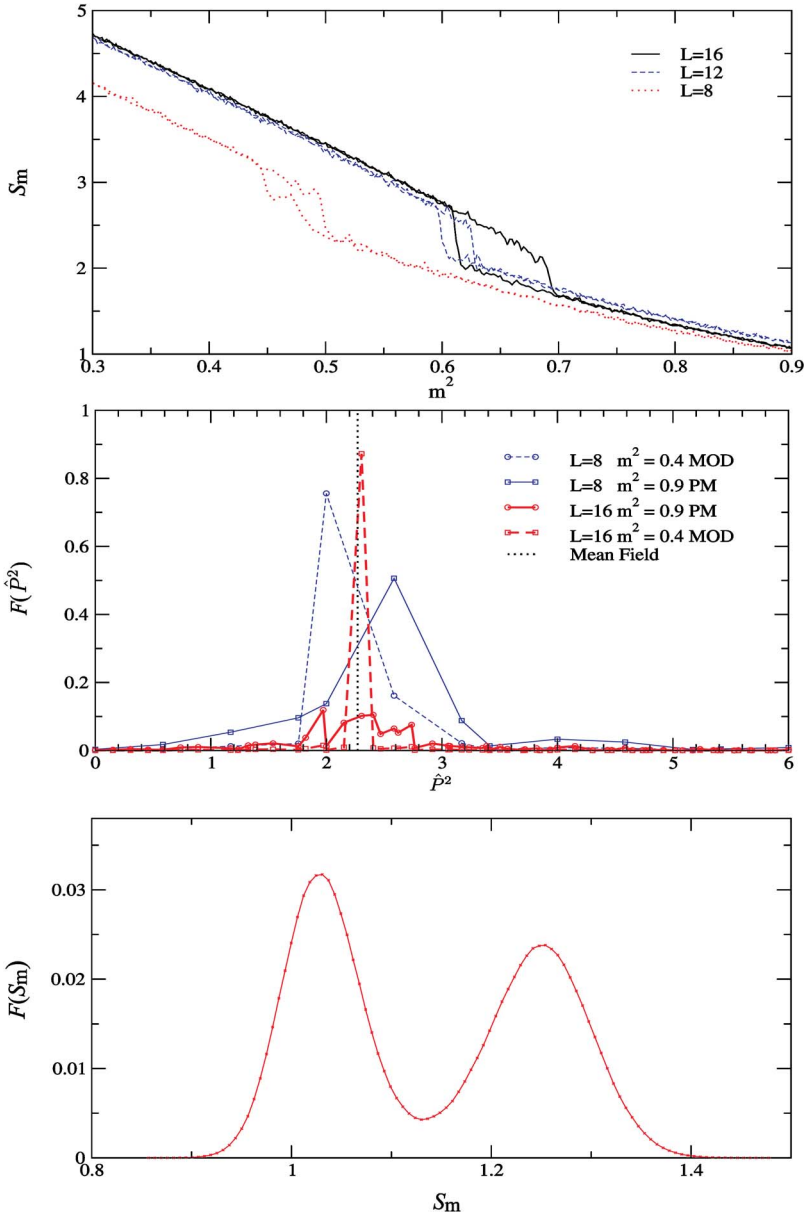

FIG. 10. (Color online) Top: Hysteresis cycle in m^2. Figure shows S_m, Eq. (38), versus m^2 for $c_2=1.5$ for lattice sizes of $L=8,12,16$. Middle: $\overline{\hat{P}^2}$ distribution at both sides of the transition for the same run as the one in the top part for the $L=8$ and $L=16$ lattices. The dotted line at $\overline{\hat{P}^2}=2.27$ is the value of $\overline{\hat{P}^2}$ predicted by mean field for this value of the parameter c_2. Bottom: Histogram of S_m for a run with fixed parameters $c_2=1.5, m^2=0.57$ in an $L=12$ lattice. The histogram shows clearly the first order character of the MOD-PM transition.

The bottom part of Fig. 10 shows the energy histogram of an $L=12$ lattice at this transition line with the characteristic double-peak of a first order transition, confirming the discontinuous character of this transition.

V. CONCLUSIONS

We have proposed and studied an effective field theoretical model which is supposed to describe the ^{4}He phase diagram around the point where solid, normal liquid, and superfluid phases meet. This model is a generalization of the *XY* model which describes the universality class of the λ transition and it is able to explain the emergence of the different phases accounting for the two-excitation dispersion relation in the superfluid phase, and to relate the apparition of a condensate at nonzero momentum (solid phase) with a continuous deformation of the phonon-roton dispersion relation when increasing the pressure (here represented by the coefficients of the higher order derivatives) at fixed temperature from the superfluid phase.

A mean field study, together with Monte Carlo simulations of this model, have been performed. The numerical simulations do not modify very much the location of the transitions in the mean field phase diagram but change in a qualitative way the nature of the transitions obtained in the mean field approximation. Both the form of the phase diagram and the order of the transitions (second-order of the *XY* universality class for the superfluid-normal liquid transition, first order for the solid-superfluid or solid-normal liquid transitions) agree with those of ^{4}He.

This model might be used as an starting point to study the possible apparition of other phases, such as a "supersolid" phase, which, after many years of debate,[18] seems to have been experimentally observed very recently[19] in the ^{4}He system.

ACKNOWLEDGMENTS

We thank J. L. Alonso for useful suggestions. This work was partially supported by Spanish MCyT FPA2001-1813 and BFM2003-08532-C02-01 research contracts, and by DGA research group program ("Biocomputation and physics of complex systems"). S.J. acknowledges financial support from DGA and from the ECHP programme, contract HPRN-CT-2002-00307, DYGLAGEMEM.

*Electronic address: jcarmona@unizar.es
†Electronic address: sergiojs@unizar.es
‡Electronic address: polonyi@fresnel.u-strasbg.fr
§Electronic address: tarancon@sol.unizar.es

[1] See, e.g., M. Le Bellac, *Quantum and Statistical Field Theory* (Oxford University Press, New York, 1992).
[2] J. A. Lipa, J. A. Nissen, D. A. Stricker, D. R. Swanson, and T. C. P. Chui, Phys. Rev. B **68**, 174518 (2003); J. A. Lipa, D. R. Swanson, J. A. Nissen, T. C. P. Chui, and U. E. Israelsson, Phys. Rev. Lett. **76**, 944 (1996); D. R. Swanson, T. C. P. Chui, and J. A. Lipa, Phys. Rev. B **46**, 9043 (1992).
[3] V. L. Ginzburg and L. P. Pitaevskiĭ, Zh. Eksp. Teor. Fiz. **34**, 1240 (1958) [Sov. Phys. JETP **7**, 858 (1958)]; V. L. Ginzburg and A. A. Sobyanin, J. Low Temp. Phys. **49**, 507 (1982); T. Fliessbach, cond-mat/0106237.
[4] M. Campostrini, A. Pelissetto, P. Rossi, and E. Vicari, Phys. Rev. B **61**, 5905 (2000).
[5] See, e.g., J. Wilks, *The Properties of Liquid and Solid Helium* (Oxford University Press, New York, 1967).
[6] R. M. Hornreich, M. Luban, and S. Shtrikman, Phys. Rev. Lett. **35**, 1678 (1975); R. M. Hornreich, J. Magn. Magn. Mater. **15-18**, 387 (1980).
[7] V. Branchina, H. Mohrbach, and J. Polonyi, Phys. Rev. D **60**, 045007 (1999).
[8] L. D. Landau, J. Phys. (Moscow) **5**, 71 (1941).
[9] H. Palevsky, K. Otnes, and K. E. Larsson, Phys. Rev. **112**, 11 (1958); J. L. Yarnell *et al.*, Phys. Rev. **113**, 1379 (1959); D. G. Henshaw and A. D. B. Woods, Phys. Rev. **121**, 1266 (1961).
[10] A. M. Ferrenberg and R. H. Swendsen, Phys. Rev. Lett. **61**, 2635 (1988).
[11] F. Cooper, B. Freedman, and D. Preston, Nucl. Phys. B **210**, 210 (1989).
[12] *Finite-Size Scaling*, edited by J. L. Cardy (North-Holland, Amsterdam, 1988).
[13] H. G. Ballesteros, L. A. Fernández, V. Martín-Mayor, A. Muñoz Sudupe, G. Parisi, and J. J. Ruiz-Lorenzo, J. Phys. A **32**, 1 (1999).
[14] H. G. Ballesteros, L. A. Fernández, V. Martín-Mayor, and A. Muñoz Sudupe, Phys. Lett. B **387**, 125 (1996).
[15] E. Bittner and W. Janke, Phys. Rev. B **71**, 024512 (2005).
[16] M. Campostrini, M. Hasenbusch, A. Pelissetto, P. Rossi, and E. Vicari, Phys. Rev. B **63**, 214503 (2001).
[17] J. L. Alonso J. M. Carmona, J. Clemente Gallardo, L. A. Fernández, D. Iñiguez, A. Tarancón, and C. L. Ullod,Phys. Lett. B **376**, 148 (1996); L. A. Fernández J. J. Ruiz-Lorenzo, M. P. Lombardo, and A. Tarancón,Phys. Lett. B **277**, 485 (1992).
[18] A. F. Andreev and I. M. Lifshitz, Sov. Phys. JETP **29**, 1107 (1969); G. V. Chester, Phys. Rev. A **2**, 256 (1970).
[19] E. Kim and M. H. W. Chan, Nature (London) **427**, 225 (2004).